



## ORIGINAL ARTICLE

# Synthesis of tetra-metal oxide system based pH sensor via branched cathodic electrodeposition on different substrates

Hisham R. Sadig<sup>a,b</sup>, Li Cheng<sup>a,\*</sup>, Teng fei Xiang<sup>a</sup>

<sup>a</sup> Nanjing University of Aeronautics and Astronautics, Material Science and Technology, Nanjing 210016, China

<sup>b</sup> Karary University, Chemical Engineering Department, Khartoum, Sudan

Received 31 August 2018; accepted 28 October 2018

Available online 9 November 2018

## KEYWORDS

Tetra-metal oxide;  
Iridium;  
Ruthenium;  
Tin;  
Titanium

**Abstract** In this paper pH sensors based on tetra-metal oxide system (TMOF) film was synthesized by branched cathodic electrodeposition technique. Four different metal oxides mainly IrO<sub>2</sub>, RuO<sub>2</sub>, SnO<sub>2</sub>, and TiO<sub>2</sub> used to form a film, which coated on various substrates such as titanium, steel, tin, and copper. The fabricated pH sensors underwent characterization and evaluation sensing performance. Characterizations results have indicated that titanium and steel substrates outperform alternative metal substrates Tin and copper. Nernstian performance of Steel and Titanium substrate with pH sensitivity ~59 mV/pH remain the same, as well as tin and copper which are behaved as super-Nernstian with sensitivity ~65 mV/pH. Fast response time ranged from 1 to 3 s were obtained. Perfect selectivity obtained using Na<sup>+</sup>, K<sup>+</sup>, Li<sup>+</sup> and Mg<sup>2+</sup> ions vs. primary one H<sup>+</sup>. © 2018 The Authors. Production and hosting by Elsevier B.V. on behalf of King Saud University. This is an open access article under the CC BY-NC-ND license (<http://creativecommons.org/licenses/by-nc-nd/4.0/>).

## 1. Introduction

PH sensors with remarkably functioning of redox reaction are used in many application including biological, chemical, materials processes, research, industrial and every request that associated with pH measurements. Up today, significant works have focused on the utilization of glass electrode, due to its excellent sensitivity, stability, and long lifetime. However, con-

cerning the practical application, the glass electrode suffers from many challenges, such as miniaturization difficulty, as well as hazardous environments including high pressure, high temperature, alkaline and hydrofluoric conditions and mechanical fragility. Therefore, solving these problems are considered as a current big challenge (O'Malley et al., 2012; Xiao-Yu and Yan, 2016).

As an alternative, various pH electrodes, such as pH sensors based on ion-sensitive field effect transistor (ISFET) sensors have the gains of planar construction, small sizes, low impedance, fast response, large-scale production ease of multi-sensor realization, and immediate use after dry storage. However, drawbacks such as a more noteworthy drift rate, the necessary of unbending encapsulation, and lower sensitivity to different pH levels Lee et al., 2009, and those differences electrodes have been reported to overcome these limitations

\* Corresponding author.

E-mail address: [licheng@nuaa.edu.cn](mailto:licheng@nuaa.edu.cn) (L. Cheng).

Peer review under responsibility of King Saud University.



Production and hosting by Elsevier

and further expand the application fields. Among them, solid-state based pH sensor (Noh et al., 2011; Olthuis et al., 1990) Numerous solid-state metal oxides considered for pH sensing electrodes, employ mostly metal wire as a substrate and are limited in their mass production and miniaturization Yao et al., 2001; Liao and Chou, 2008. Some metal oxide-based pH sensors have been developed. However, these materials exhibit hysteresis and potential drift, leading to unstable response including PtO<sub>2</sub> Kreider et al., 1995; Dario Battistel and Daniele, 2014; IrO<sub>x</sub> (El-Giar and Wipf, 2007; Huang et al., 2014; Kuo et al., 2014; da Silva et al., 2008), RuO<sub>2</sub> (Manjakkal et al., 2016; Manjakkal et al., 2014; Yang and Chou, 2012; Sardarinejad et al., 2014; Zhuiykov et al., 2016), Ta<sub>2</sub>O<sub>5</sub> (Kuo et al., 2014; Manjakkal et al., 2016), RhO<sub>2</sub>, TiO<sub>2</sub> (Manjakkal et al., 2014; Yang and Chou, 2012; Zhuiykov et al., 2016), as the pH sensing films. Among the above oxides, IrO<sub>2</sub>, RuO<sub>2</sub>, SnO<sub>2</sub> and TiO<sub>2</sub> demonstrated with more recompenses in sensor performance for various (Neil McMurray et al., 1995; Mihell and Atkinson, 1998; Kim and Yang, 2014; Bunjongprua et al., 2013; Chou and Wang, 2002).

Recently, binary metal oxide system, exhibit variety of interesting properties (Hashimoto et al., 2016; Pocrifka et al., 2006), however, still unable to get rid of singular metal oxide drawbacks such as alkaline effect, the appearance of many oxide states (which caused in super-Nernstian slopes), the cost (da Silva et al., 2008). On another side, multi-system metal oxides have attracted much attention for many applications, such as oxygen-evolving reaction electrodes, optoelectronic technology and cooling magnetic field (Terezo and Pereira, 2000; Mendes et al., 2013) owing to significant performance properties.

Numerous preparation methods used to synthesizing metal oxides, e.g. sputtering (Maurya et al., 2014; Sardarinejad et al., 2015a; Wu et al., 2011), thermal oxidation (Li et al., 2011; Wang et al., 2013), thermal decomposition (Brewer et al., 2015), electrochemical growth (Olthuis et al., 1990), screen printing (Koncki and Mascini, 1997; Neil McMurray et al., 1995), sol-gel method (Baker et al., 2007; Liao and Chou, 2009b; Islam et al., 2015; Huang et al., 2011; Manjakkal et al., 2015); Pechini method (Weber et al., 2001; Zimer et al., 2010; Zaki et al., 2012; Mashreghi and Ghasemi, 2015). Recently, electrodeposition has emerged as an alternative with perfect features candidates for oxide thin film production. Because it offers some impressive gains when compared with other methods such as sputtering, chemical deposition, etc. (i) the deposition occurs at low temperature and atmospheric pressure, (ii) it is a low-cost method which requires only simple apparatus. (iii) The film thickness can directly monitor by the charge consumed during the deposition process. The main disadvantage is that just conducting substrates can be used (Patake et al., 2009; Metikoš-Huković et al., 2006; Winiarski et al., 2016; Shmychkova et al., 2016; Pauporté et al., 2003).

Up to our knowledge, pH sensors based on tetra metal oxide that formed from the most promises candidates have not yet been thoroughly investigated. Therefore, tetraoxide film is expected to demonstrate a superior performance behavior. Motivated by these observations the objective of this paper is to examine the effect of tetra metal oxide on the PH sensing performance. Moreover, the sound effects of the substrate on the structure, chemical composition, and electrochemical performance are thoroughly considered.

In this paper, cathodic electrodeposition method is used to synthesize TMOF from IrO<sub>2</sub>, RuO<sub>2</sub>, SnO<sub>2</sub>, and TiO<sub>2</sub> on four different substrates including titanium, steel, tin and copper and used as PH sensor electrodes. The characterization tests reveal that the performance of the oxide film deposited on the Titanium and steel outperforms alternative metal substrates Tin and copper. Also, the Nernstian performance of Steel and Titanium substrate remain the same as well as tin and copper which are behaved as super-Nernstian.

## 2. Experimental

### 2.1. Preparation of substrates

Prior electrodeposition, the wire substrates titanium 0.6 mm, tin 0.5 mm, copper 0.6 mm and steel 0.5 were first mechanically polished with 600 grit SiC abrasive paper to obtained regular surface roughness. Then; chemical treatment was carried out, by using deionized water, hot 10% oxalic acid as reported elsewhere. Finally, the prepared substrates were washed and dried. For tin and copper substrate, they were used without any chemical treatment (because of the surface's corrosion reasons in the oxalic acid environment).

### 2.2. Electrodes fabrication

The electrodeposition solutions were first prepared using the method described in (Kim and Yang, 2014). 0.3 g weights of each salt (iridium chloride hydrate, ruthenium chloride hydrate, tin tetrachloride and Titanium tetrachloride) was dissolved in deionized (DI) water under magnetic stirring. After 30 min 2 mL of aqueous 30% H<sub>2</sub>O<sub>2</sub> was added to the above solution. Then 1 g of oxalic acid (C<sub>2</sub>H<sub>2</sub>O<sub>4</sub>) was added and stirred for another 30 min. pH of the solution was attuned to ~10 by a mixture of Li<sub>2</sub>CO<sub>3</sub>, Na<sub>2</sub>CO<sub>3</sub>, and K<sub>2</sub>CO<sub>3</sub> salt solution. The prepared solution was aged for one week at room temperature until its color gradually turned from light brown to black. The electrodes were then prepared by branched cathodic electrodeposition method as shown in Fig. 1. The ruthenium oxide mesh was used as the anode, while the substrates were used as a cathode with a constant current density of 4 A/dm<sup>3</sup> for 10 min under magnetic stirring condition.

## 3. Result and discussion

### 3.1. Sensor characterization

The SEM images allowed observations of the sensitive cathodic electrodeposited TMOF which deposited on the previously mentioned substrates. More details demonstrated in Fig. 2, the porous nanostructure of the film consists of homogeneously distributed, grains sized in nano-metric scale. Its size in the film ranged from 1.2 to 62.5 nm. The sensitive film is firmly adherent to the substrate it is essential to recall that measurement of the thickness done by Digital micrograph 3.7. Various thicknesses 4.83 μm, 3.9 μm, 2.5 μm, and 2.8 μm of the film coated on tin, copper, steel, and titanium electrodes respectively. Uniform elemental composition has been provided by the EDX analysis Fig. 3. Demonstrates the presence of Iridium, ruthenium, tin, and titanium in the sensitive layer.

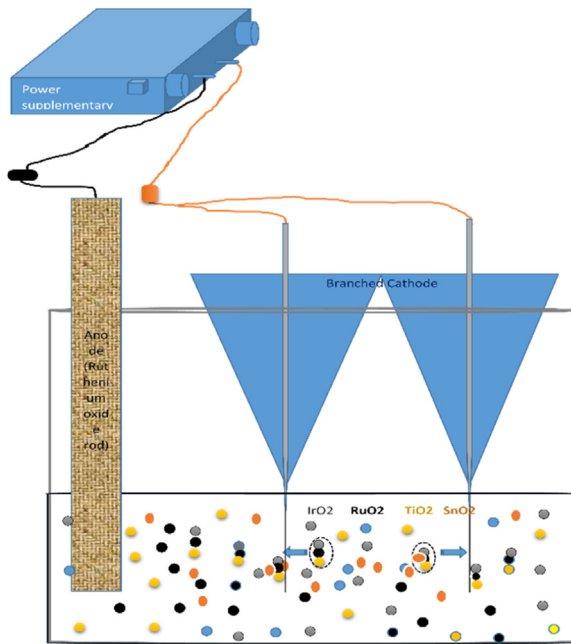


**Fig. 1** Demonstrates the deposition cell with branched cathode and ruthenium oxide anode (inert).

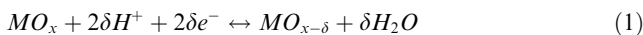
### 3.2. Sensing mechanism

The pH recognized as a measurement of hydrogen ion concentration in a solution. According to the Nernstian equation, the potential difference created between the reference and the sensitive electrodes immersed in a test solution is proportional to the pH of this solution:

$$E = E_0 - \frac{2.303RT}{nF} pH = E_0 - m.pH \quad (1)$$

where R is the gas constant, T is the temperature, F is Faraday's constant, E is the potential of the electrochemical cell and E<sup>0</sup> is the standard potential. For a single electron mechanism (n = 1), the Nernstian slope (m) is 2.303RT/nF = 59.16 mV at 25 °C. The potentiometric behavior of the sensitive electrodes was tested. Through various test solutions with known pH values the potential difference between the sensors, and the reference electrodes (calomel) was observed.

Five different explanations have been proposed to investigate the pH mechanism, those explanations have been formulated in past experiences depending on some suggested reactions. Among them, the oxygen intercalation which involved oxygen-deficient and water hydration the Eq. (1) illustrates this fact (Fog and Buck, 1984).

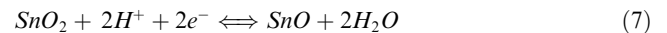
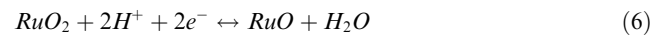
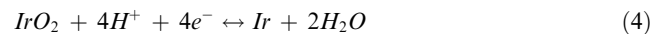
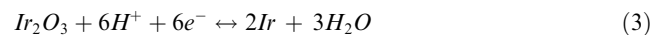


Consequently, from this reaction one can realize that the number of electrons influences the pH response. It important to note that the number of electrons is equivalent to H<sup>+</sup>, consequently, in the Nernstian equation which shown in the Eq. (2) the slope value represented the pH sensitivity and calculated to be 59.16 mV/pH. Moreover, from this calculation the difference in the number of H<sup>+</sup> and electrons (H<sup>+</sup> > e<sup>-</sup>) and (H<sup>+</sup> < e<sup>-</sup>) causes the sub and the super Nernstian behav-

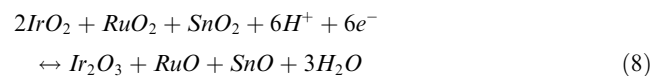
ior respectively. The super Nernstian initiated by the appearance of different oxide and hydroxide states which cause the mixed potential, also existent of different oxidized and reduced metal oxide (Olthuis et al., 1990; Sardarinejad et al., 2015a; Ges et al., 2005). For the sensitivity below than 59.16 mV/pH, the redox reaction could characterize by the transfer of more than one electron per proton and vice versa in super-Nernstian (Pocrifka et al., 2006; Huang et al., 2011).

$$E = E^0 - 2.303 \frac{RT}{nF} pH = E^0 - 59.16 pH \quad (2)$$

In this experiment, the case of IrO<sub>2</sub>-RuO<sub>2</sub>-SnO<sub>2</sub>-TiO<sub>2</sub> composition, all of IrO<sub>2</sub>, RuO<sub>2</sub>, and SnO<sub>2</sub> are the oxides which act as the more responsible for sensing mechanism (Pocrifka et al., 2006; Huang et al., 2011; Manjakkal et al., 2015). IrO<sub>2</sub>, RuO<sub>2</sub>, and SnO<sub>2</sub> are a mixed electronic and ionic conductor with the stable rutile structure. In the general point of view, when IrO<sub>2</sub>, RuO<sub>2</sub>, and SnO<sub>2</sub> are exposed to a solution, the reaction of H<sup>+</sup> and OH<sup>-</sup> ions provides a partial transition of Ir, Ru(IV) and Sn to Ir, Ru(III) and Sn(III) respectively, that formation of a couple of higher and lower valence metal oxides illuminated in (Fog and Buck, 1984; Glab et al., 1989). More explanation is given in the Eqs. (3)–(5) for iridium. Also Eq. (6) for ruthenium. While Eq. (7) Represented the redox reaction of the tin oxide



From all those equations the Eq. (5) have been represented for other sensor which behaved as the nernstian in (Ges et al., 2005), it is the most suitable equation to be taken as the standard to describe the current electrodes especially for titanium and stainless steel. Eq. (6) demonstrated for Ru and Eq. (7) for tin oxide. Here, it important to reminder that almost of Ru and Sn oxides provide a sub-Nernstian mannered electrodes, however, anhydrous Ir oxide encourages the super-Nernstian due to existent of different oxidation states. Accordingly, in this work gathering two different manner in one system have significant impact towards Nernstian manner, so one can contributes that, the most dominant reaction that can predict the TMOF behavior is the total reaction which illustrated below in the Eq. (8).



Up to our knowledge, there is not any reaction suggested for pH sensing for TiO<sub>2</sub>. However, various reports experimentally described the sub-Nernstian response for this oxide. In addition to that, it has been used in combination with other oxides to form a binary system for reducing the cost of other expensive metal oxides, without affecting the sensitivity (Manjakkal et al., 2015). From the Eq. (8) and the of data pH sensitivity received from the experiment ~59 for titanium and stainless steel ~65 for both of copper and tin, we can conclude that our as-prepared film participated in Nernstian

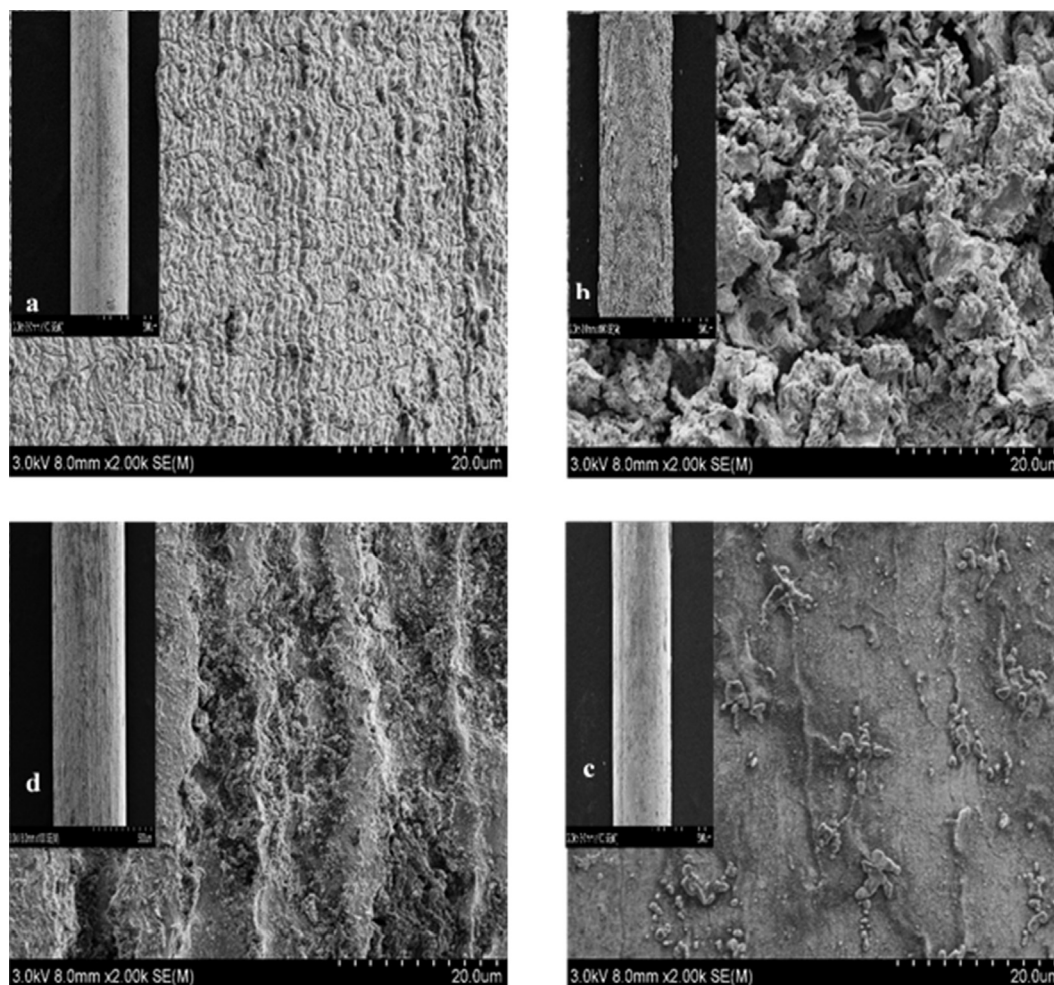


**Fig. 2** Demonstrates the SEM images of fine part of coated electrodes and the corresponding TM film (a) copper substrates, (b) tin substrates (c) steel wire, and (d1, d2 for Titanium wire).

reaction. So there is equivalent in the number electrons and  $H^+$  transfer in our system reaction as it is clear from the Eq. (8) In the case of titanium and stainless steel. Conversely remarked super-Nernstian behavior in copper and tin substrates, this can contribute to the kind of substrates, commonly the tin and copper affected by acids.

In acidic solutions, protons are released by dissociative adsorption of water, the surface of metal oxide develops protonated, and the electrode potential increases with increasing of pH (Kurzweil, 2009). In basic solutions, the surface of metal oxide turns out to be negatively charged by the freeing of  $OH^-$  groups by the water dissociative adsorption. As a result, the electrode potential decreases with rising pH in the basic region (Kurzweil, 2009). Initially, a series of potentiometric measurements were carried out to evaluate the sensitivity, response time and stability of the fabricated tetra-system film electrode versus an external glass reference electrode.

The dynamic response of the sensitive electrodes versus glass reference electrode at stabilized points for various pH of the solutions is presented in Fig. 4. The measured potential values of the sensor were plotted vs. the various pH solutions, it can be realized from this figure that the open circuit potential

decreases with the increasing pH. Consequently this confirms that the pH sensitivity of the prepared electrode was changed according to the pH change of the solutions. Experimental values of the potential were found to be almost an entirely linear function of pH. According to the Nernst relationship, the E potential of the fabricated sensors is the following function of the pH of a solution.

Hence, at room temperature, the slopes of the fabricated sensors for titanium and stainless steel were  $\sim 59$  so those values were matched the Nernstian slope, and were closer to the theoretical factor of 59.16 mV/pH. Moreover, they were higher than the values 56.9 reported in (Zimer et al., 2010) and 56.03 mV/pH described by Pocrifka et al. (2006). for a thin film of  $RuO_2-TiO_2$  prepared using the Pechini method and deposited on a titanium substrate. Also found higher than slope provided by Pt-doped nanostructured  $RuO_2$  sensing electrode described by Zhuiykov (2009), which exhibits a sensitivity of 58 mV/pH, the fabricated stainless steel sensor shows a typical Nernstian slope provided by Kuo et al. (2014). While the tin and copper electrodes similar to that super Nernstian slope which have been obtained by Tomi Ryyänen et al. (2010). The super Nernstian behavior that occurred in both

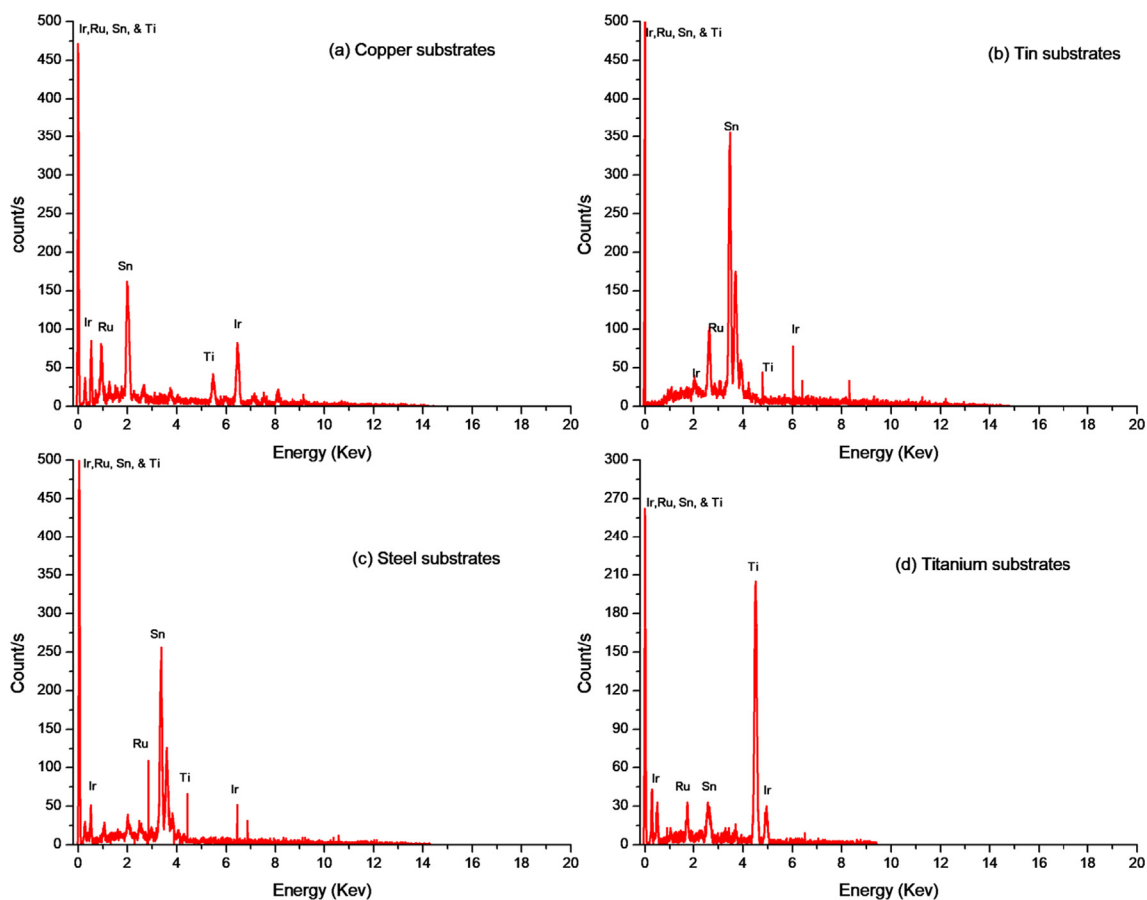


**Fig. 3** Show the EDS elemental analysis of fabricated films on the different substrates (a) copper, (b) tin, (c) steel, and (d) titanium.

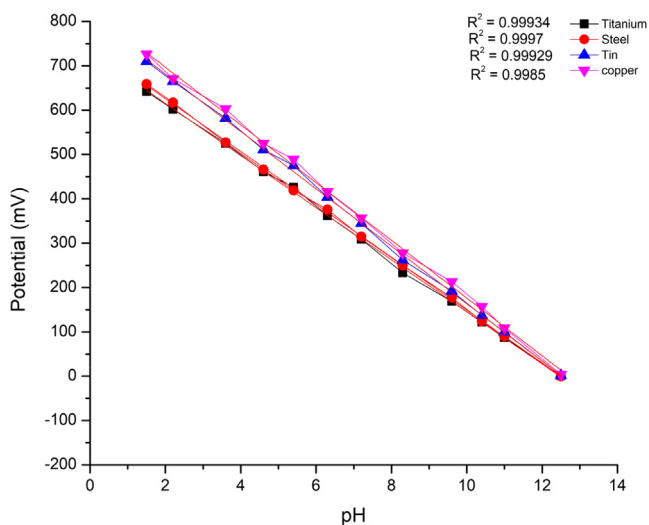


**Fig. 4** Show the sensitivity of the fabricated electrodes (Tin, Copper, Steel, and Titanium).

tin and copper electrodes can contribute to the fact of different metal oxides' oxidation states appearance during the redox reactions as it described in a previous research (Ges et al., 2005), besides, the type of substrates, (tin and copper) which

were lack of a such characteristics, and this may be due to the reaction of the acidic solution with these substrates thorough some existent pores.

### 3.2.1. Sensitivity, and the rate of drift

The validation of the stability of pH sensor fabricated in this work, implemented by immersing all coated wire in different test solutions for 10 min, this step repeated three times, for each 10 min interval, the pH was periodically measured out of the testing time and estimated at 20 s. After each 10 min test, the sensor cleaned with DI water followed by drying with compressed air. The procedure results demonstrated In Fig. 4 the averagely potential value of the three tests plotted versus time for different pH values ranged between 1.5 pH–pH 12.5 and different electrodes. A remarkable stable output potential obtained for all pH values. However, the behavior of super-Nernstian detected in tin and copper electrodes, as well as, similarity Nernstian observed in titanium and steel electrodes.

To categorize factors affecting the performance of the pH sensors, a real and long-term pH measurement should be arranged. Accordingly, this circumstance give rise to the drift effect of the sensing device, from our knowledge, potential drift defined as the difference between the peak potential value and the 90% value of the full potential (Huang et al., 2011). Therefore, it is considered the source of pH measurement errors that impact the resolution and accuracy of the pH sensor. Thus it could not be ignored, especially in long-term pH

monitoring. The potential drift typically caused by dynamic processes, such as ion neutralization also known as the effect of liquid junction potential, porosity variation and surface rehydration (Yao et al., 2001; Liao and Choua, 2008), also attributed to the diffusion and trapping of hydrogen and hydroxide ions through the pores and the boundaries sensing electrodes (Sardarinejad et al., 2014). In the current experimental, the drift was potential change with time, and was defined as the output voltage of all fabricated electrodes. Confirmation data illustrated in (Table 1). Our TMOF has a low rate of drift estimated between 0.7 and 5 mV/h for all made electrodes; this value was very significant when compared by almost of others reported in (Liao and Chou, 2009a).

### 3.2.2. Reversibility, hysteresis, and time response

The investigation pH sensor reversibility carried out by switching pH electrodes sequentially between different pH ranged 1.5–12.5 buffer solutions in forward and backward orders at 240 s intervals without cleaning or drying the pH sensor, and the measured potential versus time monitored. The switching cycle repeated three times. Fig. 5 illustrated the averagely recorded potentials (averaged over three tests) for TMOF thin film. A conventional pH sensor was used to obtain reference pH values during the monitoring processes using HCl/KOH solutions. The average pH sensitivities for both cases in the acid-to-base and vice versa were around 59 mV/pH for titanium and steel electrodes, while were approximately 65 mV/pH with correlation coefficients over 0.99. The potential variations at each pH level were less than seven mV of the standard deviation. Fig. 5 demonstrate the experimental results, excellent reversibility and stable pH sensors' response to the same behavior of Nernstian for titanium and steel electrode. While in parallel side tin and copper were same as super-Nernstian performed. One can contribute this behavior to the conductivity of (tin and copper) and influence of adding HCl to attuning the pH of the solutions in those metal oxide this acid inter through the pores in the shelf that covers the electrode and

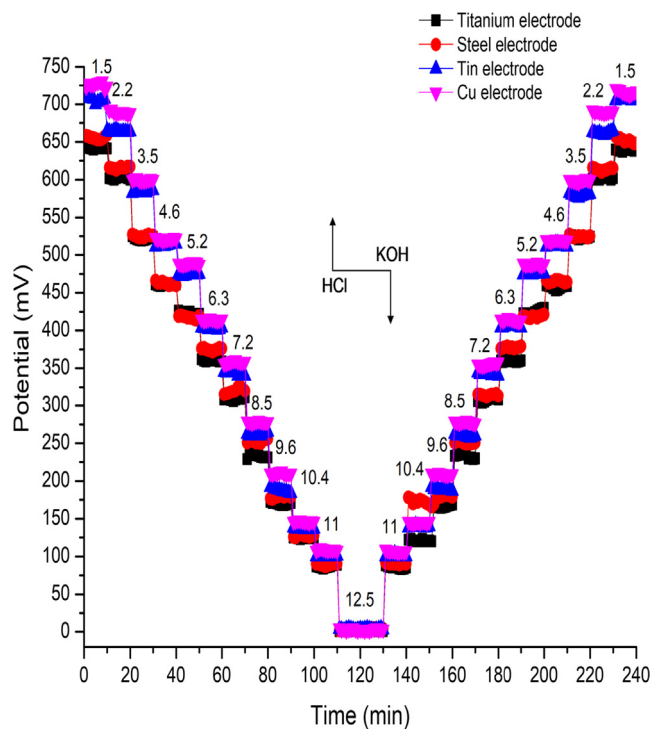


Fig. 5 Show the reversibility TMOF film of titanium, steel, tin electrodes, and copper.

make some side-reactions. Moreover, existent of the various oxidation states also effected towards super-Nernstian manners (Bezbaruah and Zhang, 2002).

It is essential to consider the hysteresis phenomena, for its role in the inhibition of the resolution of the sensor. The hysteresis of TMOF films tests runs have been taken twice through pH 2.2, pH 3.5, pH 7.2, and pH 9.6. As a result, hysteresis well-defined as the difference between first and second

Table 1 Illustrates the rate of drift, saturated potentials, and peak potentials for all fabricated electrodes.

Type of substrate	pH	Saturated potential (mV)	Peak potential (mV)	Rate of drift (mv/h)
Ti	2.2	602.2	605	2.8
	3.5	521.7	525	3.3
	7.2	308.0	311	3.0
	9.6	170.0	172.0	2.0
Steel	2.2	616.1	617	1.1
	3.5	524.6	527	2.4
	7.2	223.2	325	1.8
	9.6	179.3	182	2.7
Tin	2.2	664.3	665	0.7
	3.5	584.6	586	1.4
	7.2	343.0	346	3.0
	9.6	188.0	193	5.0
Copper	2.2	689.6	693	3.4
	3.5	599.6	602	2.4
	7.2	358.5	360	1.5
	9.6	210.4	213	2.6

**Table 2** Shows the hysteresis width for all electrodes (calculated using measurement of test 1, and test 2).

Type of substrate	pH	Test No 1 potential (mV)	Test No 2 potential (mV)	Hysteresis width (mv)
Ti	2.2	602.2	601.5	0.7
	3.5	521.7	523.3	1.6
	7.2	308.9	307.4	-1.5
	9.6	170.0	161.9	8.1
Steel	2.2	615.6	613.6	2.0
	3.5	525.2	524.6	0.6
	7.2	319.9	314.2	5.7
	9.6	179.3	177	2.3
Tin	2.2	664.1	653.6	-10.5
	3.5	584.6	579.2	5.4
	7.2	343.1	342.3	0.8
	9.6	188.0	189.5	-1.5
Copper	2.2	689.6	690	-0.4
	3.5	599.8	598.9	0.9
	7.2	358.5	355.7	2.8
	9.6	210.4	209.3	1.1

run, as it appears by the demonstrative data in the (Table 2), insignificant hysteresis provided by the TMOF film compared by some values reported in (Maurya et al., 2014; Liao and Chou, 2009a) (see Table 3).

According to the literature, the response time of a pH sensor defined as the transit time required for its potential to reach 90% of an equilibrium value after immersing the sensor in test solution (Sardarinejad et al., 2015a, 2015b). The response time of TMOF sensing electrodes studied by continuous testing. The as-prepared electrodes were tested in each pH buffer for about 10 s and immediately transferred into the next pH buffer without rinsing with deionized water or drying. The potentials between the electrodes of the developed pH sensors recorded at ~10 s intervals for buffer solutions of pH 1.5, pH 6.3 and pH 10.4 at 19 °C. The response time for each sensor calculated from the average of three test run. Fig. 6 shows the response times for titanium, steel, tin, and copper. The response times in pH 6.3 and pH 10.4 were 1.8 s, and 1 s, respectively; for almost electrodes, except for tin which response times were 3 s and 1.2 s correspondingly to mentioned pH. Comparing reversibility, hysteresis, and time response of TMOF with previous oxide film reported in other works (Yao et al., 2001; Islam et al., 2015) found that it has perfect reversibility with negligible hysteresis and fast response time.

### 3.2.3. Reproducibility

Reproducibility is one of the essential characteristics when considering sensor development, which realized by getting consistent sensor sensitivity. Four TMOF electrodes made by different wires, but the same fabrication process used to confirm reproducibility formations demonstrated in Fig. 7. Potentials for all electrodes obtained in the same pH solution measuring in the acid-to-base direction. A conventional reference electrode used to ensure the same reference potential for each electrode. The potential deviations for the TMOF electrodes investigated. And Found less than 7 mV, and the sensitivities obtained from the averaged potentials were around 59 mV/pH for titanium and steel and about 65 mV/pH for tin and copper. The responses were almost overlapped, indicating excellent reproducibility, with a correlation coefficient higher than 0.999. The measurement is done by sharply changing the pH from 1.5 to 12.5.

### 3.2.4. Temperature and interference effect on the pH sensor

Fundamentally, the Nernstian potential and interference factor are temperature dependent, as shown in Eq. (6), that the potential E-E0 is directly proportional to the temperature T in the Nernstian equation. The temperature dependence of our TMOF pH sensor investigated in different buffer solutions

**Table 3** The temperature corresponding sensitivity of the TMOF electrodes.

Temperature °C	Slope of titanium electrodes	Slope of Tin electrodes	Slope of titanium electrodes	Slope of titanium electrodes
10	-57.2	-58.2	-62.3	-63.2
15	-57.8	-58.6	-62.9	-63.5
20	-57.9	-58.8	-63.4	-64.7
25	-58.7	-58.8	-64.4	-65.1
30	-59.6	-59.5	-64.8	-65.7
35	-59.1	-59.7	-65	-65.6
40	-59.2	-59.9	-65.1	-66.2
45	-59.3	-60.1	-65.2	-66.5

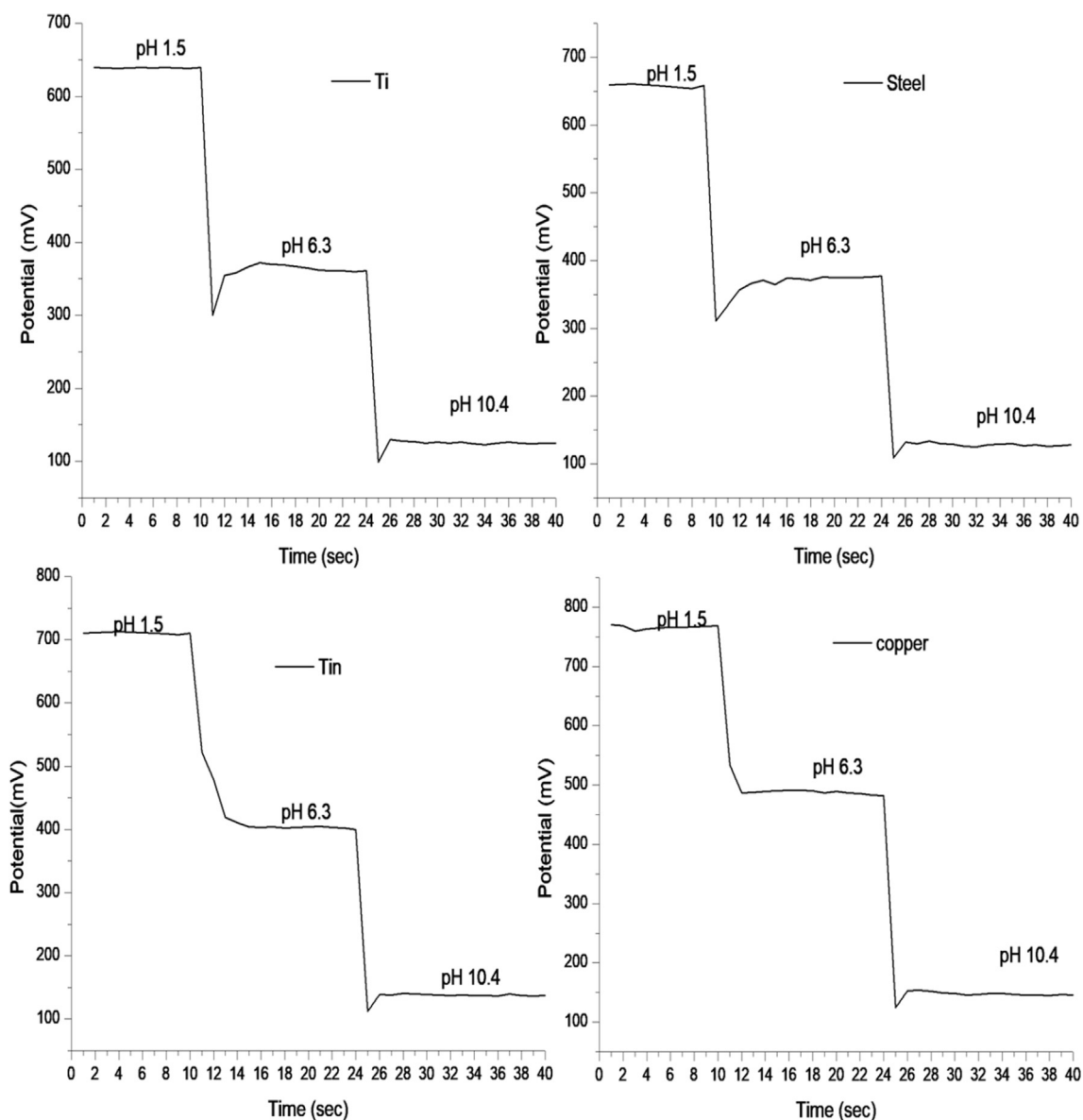
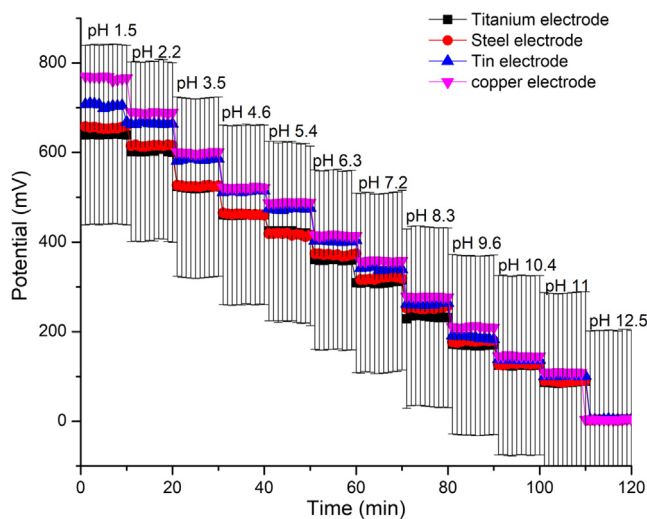


Fig. 6 Represents the dynamic response time of titanium, steel, and tin electrodes.

(2.2, 3.5, 4.6, 5.4, 7.2, 9.7, and 10.5). The measurements recorded through eight temperatures 10, 15, 20, 25, 30, 35, 40, and 45 °C, this achieved by using silicon-oil bath assisted by thermometer for reading the targeted temperature degrees. The sensor cleaned with DI water and air dried between tests in different solutions. Our pH sensors, expected with a temperature dependence corresponding to the Nernstian Eq. (6). The temperature dependence and sensitivity affected shown in Fig. 8. The measured temperature coefficients of the sensitivity of titanium, steel, tin, and copper were 0.062 mV/pH °C, 0.053 mV/pH °C, 0.086 mV/pH °C, and 0.095 mV/pH °C, respectively. These values is very significant when compared with the values described in Sardarinejad et al. (2015b), and according to the performance of the electrodes they seem to act as normal as common electrodes. More detailed data demonstrated in (Table 4) from the data presented for temper-

ature affect the consistency of TMOF temperature dependency matched with the theory.

The cation interferences of the TMOF selectivity were conducted with the fixed interference method in pH measurements. According to the Nikolsky–Eisenman equation (Pungor et al., 1975–1977; Umezawa et al., 2000), the interference effects from different ions ( $\text{Na}^+$ ,  $\text{K}^+$ ,  $\text{Li}^+$ ,  $\text{Mg}^{2+}$ ) were calculated with the potentiometric selective coefficients in the mentioned equation. The cations were used to compare the interference effects in potentiometric measurements of the selectivity coefficient. The interference cation agents (0.1 M of NaCl, 0.1 M of KCl, 0.1 M of LiCl and 0.1 M of  $\text{MgCl}_2$ ) were added separately into four sample solutions at different pH levels of a test buffer solution. The sensitivity was measured before, and after the interference agent was added at room temperature. The presence of the cations  $\text{K}^+$ ,  $\text{Na}^+$ ,



**Fig. 7** Explain the reproducibility of fabricated electrodes (titanium, steel, tin and copper).

$\text{Li}^+$  and  $\text{Mg}^{2+}$  changed slightly the sensitivity slopes of the fabricated sensors as shown in the Table 4. The selectivity coefficients for cations were calculated and the supporting data given in (Table 5).

### 3.2.5. The life time of the TOMF

The determination of our TOMF life time carried out through 3 months, by immersing the fabricated electrodes in different pH ranged from 1 to 12 solutions. Four different runs done within weeks to obtain four different potentials, then average values calculated. For every month the sensitivity obtained by plotting received potentials vs. corresponding pH. The detailed information supplied in the (Table 6). From this table it is clear that all fabricated electrodes films have keep the same stability from the first month till the third month, however, in the last week of third month the real sensitivity change has initiated probably for the storage condition of the electrodes were not the ideal one. Besides, experimental

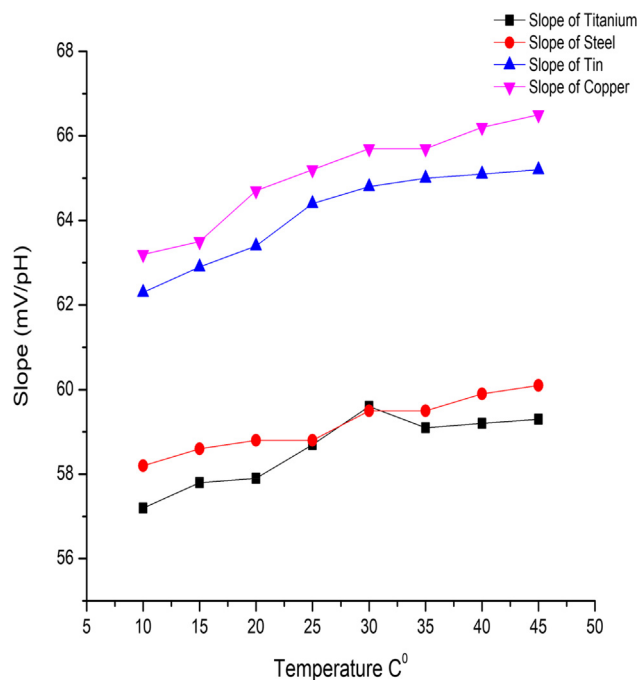


**Fig. 8** Temperature effect in TMOF sensitivity, for all electrodes (titanium, steel, tin, and copper).

**Table 6** Show the life time of the fabricated electrodes.

Type of electrode	Sensitivity/month		
	First month	Second month	Third month
Titanium	59.00	59.00	58.50
Steel	59.60	59.60	59.40
Tin	64.7	67.6	67.4
Copper	65.05	65.30	65.41

exhausting-usage of the electrodes. So the life time of the electrodes was 3 months this period was acceptable comparing with (Sadig et al., 2018).

**Table 4** Show the deviation of the TMOF sensitivity slope by interference effect.

Substrates	The slope without interference	Slope in $\text{K}^+$	Slope in $\text{Na}^+$	Slope in $\text{Li}^+$	Slope in $\text{Mg}^{2+}$
Titanium	58.6	58.55	58.54	58.51	58.49
Steel	60.1	60.04	60.05	60.03	60.01
Tin	63.13	63.10	63.109	63.12	63.1
Copper	70.139	70.13	70.127	70.13	70.09

**Table 5** Demonstrates the selectivity of TMOF film of the different substrates.

Substrates	Selectivity coefficient of $\text{K}^+$	Selectivity coefficient of $\text{Na}^+$	Selectivity coefficient of $\text{Li}^+$	Selectivity coefficient of $\text{Mg}^{2+}$
Titanium	$1.21 \times 10^{-17}$	$1.21 \times 10^{-17}$	$5.04 \times 10^{-24}$	$1.05 \times 10^{-44}$
Steel	$5.98 \times 10^{-16}$	$2.94 \times 10^{-14}$	$1.35 \times 10^{-14}$	$6.81 \times 10^{-35}$
Tin	$4.2 \times 10^{-16}$	$3 \times 10^{-16}$	$2.2 \times 10^{-16}$	$3.1 \times 10^{-30}$
Copper	$4.14 \times 10^{-4}$	$4.2 \times 10^{-4}$	$8.4 \times 10^{-6}$	$1.7 \times 10^{-7}$

#### 4. Conclusion

In this work, new tetra – metal oxide based film adhesives developed and applied for pH sensing electrodes. Potentiometric pH sensors fabricated on different substrates such as titanium, steel, tin, and copper by cathodic electrodeposition.

Furthermore, modification of the cathode successfully utilized by using branched cathode for development and saving time in coating more than one wire at the same time. EDX analysis revealed the elemental composition of the film with nanometric porous and micro-metric thickness of TMOF. SEM investigations show the uniform tetra composition, the porous and fine-grained nanostructure of the sensing electrode. Applying a wide pH range (1.5–12.5) potentiometric analysis indicates that the sensitivity of TMOF film is close to the ideal Nernstian response for titanium and steel wires, while it was super-Nernstian in tin and copper case. The drift and hysteresis effects have no significant impact on the sensing performance. All fabricated sensors exhibit speedy response and acceptable reproducibility, temperature dependency and perfect selectivity. In addition to other characteristics the life time of the electrodes investigated and found to be 3 month in a harsh environment. The fabricated pH sensor especially the TMOF coated on titanium and steel can be miniaturized and applied in water quality and environmental monitoring, chemical and biological labs, and in vivo clinical tests.

#### Acknowledgment

This work funded and supported by – Material science and technology college- Nanjing University of Aeronautics and Astronautics in China. Authors would like to appreciate the funder and supporter. Also thanks to Karary University-Sudan for their support.

#### References

- Baker, P.G.L., Sanderson, R.D., Crouch, A.M., 2007. Sol-gel preparation and characterisation of mixed metal tin oxide thin films. *Thin Solid Films* 515, 6691–6697.
- Bezbaruah, Achintya N., Zhang, Tian C., 2002. Fabrication of anodically electrodeposited iridium oxide film pH microelectrodes for microenvironmental studies. *Anal. Chem.* 74, 5726–5733.
- Brewer, Paul J., Leach, A.S., Brown, Richard J.C., 2015. The role of the electrolyte in the fabrication of Ag/AgCl reference electrodes for pH measurement. *Electrochim. Acta* 161, 80–83.
- Bunjongprua, W., Porntheeraphat, S., Rayanasukh, Y., Pankiewa, A., 2013. Very low drift and high sensitivity of nanocrystal TiO<sub>2</sub> sensing membrane on pH-ISFET fabricated by CMOS compatible process. *Appl. Surf. Sci.* 267, 206–211.
- Chou, Jung Chuan, Wang, Yii Fang, 2002. Preparation and study on the drift and hysteresis properties of the tin oxide gate ISFET by the sol-gel method. *Sens. Actuat. B* 86, 58–62.
- da Silva, G.M., Lemos, S.G., Pociřka, L.A., Marreto, P.D., Rosario, A.V., Pereira, E.C., Rosario, A.V., Pereira, E.C., 2008. Development of low-cost metal oxide pH electrodes based on the polymeric precursor method. *Anal. Chim. Acta* 616, 36–41.
- Dario Battistel, G.B., Daniele, Salvatore, 2014. Platinum/alumina thin films prepared by r.f. magnetron sputtering as platforms in voltammetric sensing. *Sens. Actuat. B* 191, 143–151.
- El-Giar, Emad El-Deen M., Wipf, David O., 2007. Microparticle-based iridium oxide ultramicroelectrodes for pH sensing and imaging. *J. Electroanal. Chem.* 609, 147–154.
- Fog, Agner, Buck, Richard P., 1984. Electronic semiconducting oxides as pH sensors 5, 137–146.
- Ges, Igor A., Ivanov, Borislav L., Schaffer, David K., Lima, Eduardo A., Werdich, Andreas A., Baudenbacher, Franz J., 2005. Thin-film IrOx pH microelectrode for microfluidic-based microsystems. *Biosens. Bioelectron.* 21, 248–256.
- Glab, S., Hulanicki, Adam, Edwall, Gunnar, Ingman, Folke, 1989. Metal-metal oxide and metal oxide electrodes as pH sensors, 21, 29–47.
- Hashimoto, T., Miwa, Mariko, Nasu, Hiroyuki, Ishihara, Atsushi, Nishio, Yuji, 2016. pH sensors USING 3d-block metal oxide-coated stainless steel electrodes. *Electrochim. Acta* 220, 699–704.
- Huang, Wen-Ding, Cao, Hung, Deb, Sanchali, Chiao, Mu, Chiao, J. C., 2011. A flexible pH sensor based on the iridium oxide sensing film. *Sens. Actuat. A* 169, 1–11.
- Huang, Xiao-rong, Ren, Qiong-qiong, Yuan, Xiao-jun, Wen, Wei, Chen, Wei, Zhan, Dong-ping, Chen, Wei, Zhan, Dong-ping, 2014. Iridium oxide based coaxial pH ultramicroelectrode. *Electrochem. Commun.* 40, 35–37.
- Islam, Shumaila, Bidin, Noriah, Riaz, Saira, Rahman, Rosly A., Naseem, Shahzad, Marsin, Faridah Mohd, 2015. Mesoporous SiO<sub>2</sub>-TiO<sub>2</sub>nanocomposite for pH sensing. *Sens. Actuat., B* 221, 993–1002.
- Kim, Tae Yong, Yang, Sung, 2014. Fabrication method and characterization of electrodeposited and heat-treated iridium oxide films for pH sensing. *Sens. Actuat. B* 196, 31–38.
- Koncki, Robert, Mascini, Marco, 1997. Screen-printed ruthenium dioxide electrodes for pH measurements. *Anal. Chim. Acta* 351, 143–149.
- Kreider, Kenneth G., Tarlov, Michael J., Cline, James P., 1995. Sputtered thin-film pH electrodes of platinum, palladium, ruthenium, and iridium oxides. *Sens. Actuators, B* 28, 167–172.
- Kuo, Li-Min, Chou, Yi-Chia, Chen, Kuan-Neng, Chien-Chia, Lu., Chao, Shuchi, 2014. A precise pH microsensor using RF-sputtering IrO<sub>2</sub> and Ta<sub>2</sub>O<sub>5</sub> films on Pt-electrode. *Sens. Actuat., B* 193, 687–691.
- Kurzweil, Peter, 2009. Metal oxides and ion-exchanging surfaces as pH sensors in liquids: state-of-the-art and outlook. *Sensors* 9, 4955–4985.
- Lee, Chang-Soo, Kim, Sang Kyu, Kim, Moonil, 2009. Ion-sensitive field-effect transistor for biological sensing. *Sensors* 9, 7111–7131.
- Li, Xiaopeng, Zhiyong, Gu., Cho, JungHwan, Sun, Hongwei, Kurup, Pradeep, 2011. Tin-copper mixed metal oxide nanowires: synthesis and sensor response to chemical vapors. *Sens. Actuat. B* 158, 199–207.
- Liao, Yi-Hung, Chou, Jung-Chuan, 2009a. Fabrication and characterization of a ruthenium nitride membrane for electrochemical pH sensors. *Sensors* 9, 2478–2490.
- Liao, Yi-Hung, Chou, Jung-Chuan, 2009b. Preparation and characterization of the titanium dioxide thin films used for pH electrode and procaine drug sensor by sol-gel method. *Mater. Chem. Phys.* 114, 542–548.
- Liao, Yi-Hung, Chou, Jung-Chuan, 2008. Preparation and characteristics of ruthenium dioxide for pH array sensors with real-time measurement system. *Sens. Actuat., B* 128, 603–612.
- Manjakkal, Libu, Cvejın, K., Kulawik, Jan, Zarask, Krzysztof, Szwagierczak, Dorota, Socha, Robert P., 2014. Fabrication of thick film sensitive RuO<sub>2</sub>-TiO<sub>2</sub> and Ag/AgCl/KCl reference electrodes and their application for pH measurements. *Sens. Actuat. B* 204, 57–67.
- Manjakkal, Libu, Cvejın, K., Kulawik, Jan, Zaraska, Krzysztof, Szwagierczak, Dorota, Stojanovic, Goran, 2015. Sensing mechanism of RuO<sub>2</sub>-SnO<sub>2</sub> thick film pH sensors studied by potentiometric method and electrochemical impedance spectroscopy. *J. Electroanal. Chem.* 759, 82–90.
- Manjakkal, Libu, Cvejın, Katarina, Kulawik, Jan, Zaraska, Krzysztof, Socha, Robert P., Dorota Szwagierczak, D., 2016. X-ray photoelectron spectroscopic and electrochemical impedance spectroscopic analysis of RuO<sub>2</sub>-Ta<sub>2</sub>O<sub>5</sub> thick film pH sensors. *Anal. Chim. Acta* 931, 47–56.

- Mashreghi, A., Ghasemi, M., 2015. Investigating the effect of molar ratio between TiO<sub>2</sub> nanoparticles and titanium alkoxide in Pechini based TiO<sub>2</sub> paste on photovoltaic performance of dye-sensitized solar cells. *Renew. Energy* 75, 481–488.
- Maurya, D.K., Sardarinejad, A., Alameh, K., 2014. Recent developments in R.F. magnetron sputtered thin films for pH sensing applications—an overview. *Coatings* 4, 756–771.
- Mendes, A.C., Maia, L.J., Paris, E.C., Li, M. Siu, 2013. Solvent effect on the optimization of 1.54 μm emission in Er-doped Y<sub>2</sub>O<sub>3</sub>-Al<sub>2</sub>O<sub>3</sub>-SiO<sub>2</sub> powders synthesized by a modified Pechini method. *Curr. Appl. Phys.*, 13, 1558–1565.
- Metikos-Huković, M., Babić, R., Jović, F., Grubač, Z., 2006. Anodically formed oxide films and oxygen reduction on electrodeposited ruthenium in acid solution. *Electrochim. Acta* 51, 1157–1164.
- Mihell, J.A., Atkinson, J.K., 1998. Planar thick-film pH electrodes based on ruthenium dioxide hydrate. *Sens. Actuat.*, B 48, 505–511.
- Neil McMurray, H., Douglas, P., Abbot, Duncan, 1995a. Novel thick-film pH sensors based on ruthenium dioxide-glass composites. *Sens. Actuat. B* 28, 9–15.
- Neil McMurray, H., Douglas, Peter, Abbot, Duncan, 1995b. Novel thick-film pH sensors based on ruthenium dioxide-glass composites. *Sens. Actuat. B* 28, 9–15.
- Noh, Jongmin, Park, Sejin, Boo, Hankil, Kim, Hee Chan, Chung, Taek Dong, 2011. Nanoporous platinum solid-state reference electrode with layer-by-layer polyelectrolyte junction for pH sensing chip. *Lab Chip* 11 (4), 664–671.
- O'Malley, Matthew J., Woodwarda, Patrick M., Verweij, Henk, 2012. Production and isolation of pH sensing materials by carbonate melt oxidation of iridium and platinum. *J. Mater. Chem.* 22 (16), 77–82.
- Olthuis, W., Robben, M.A., Bergveld, P., 1990. pH sensor properties of electrochemically grown iridium oxide. *Sens. Actuat. B* 2, 247–256.
- Patake, V.D., Lokhande, C.D., Joo, Oh Shim, 2009. Electrodeposited ruthenium oxide thin films for supercapacitor: effect of surface treatments. *Appl. Surf. Sci.* 255, 4192–4196.
- Pauporté, Th., Goux, A., Kahn-Harari, A., de Tacconi, N., Chen-thamarakshan, C.R., Rajeshwar, K., Lincot, D., 2003. Cathodic electrodeposition of mixed oxide thin films. *J. Phys. Chem. Solids* 64, 1737–1742.
- Pocrifka, L.A., Gonçalves, C., Grossi, P., Colpa, P.C., Pereira, E.C., 2006. Development of RuO<sub>2</sub>-TiO<sub>2</sub> (70–30) mol% for pH measurements. *Sens. Actuat. B* 113, 1012–1016.
- Pungor, E., Toth, K., Hrabeczy-Pall, A., 1975–1977. Selectivity coefficients of ion-selective electrodes. *Pure Appl. Chem.* 51, 1913–1980.
- Sadig, Hisham, R., Cheng, Li., Xiang, T., 2018. Using sol-gel supported by novel economic and environment-friendly spray-coating in the fabrication of nanostructure tri-system metal oxide-based pH sensor applications. *J. Electroanal. Chem.* 827, 93–102.
- Sardarinejad, A., Maurya, D.K., AlamehElectron, K., 2014. The effects of sensing electrode thickness on ruthenium oxide thin-film pH sensor. *Sens. Actuat. A* 214, 15–19.
- Sardarinejad, Ali, Maurya, Devendra Kumar, Alameh, Kamal, 2015a. The pH sensing properties of RF sputtered RuO<sub>2</sub> thin-film prepared using different Ar/O<sub>2</sub> flow ratio. *Mater. Chem. Phys.* 8, 3352–3363.
- Sardarinejad, A., Maurya, D.K., Khaledb, M., Alameh, K., 2015b. Temperature effects on the performance of RuO<sub>2</sub> thin-film pH sensor. *Sens. Actuat. A* 233, 414–421.
- Shmychkova, O., Luk'yanenko, T., Amadelli, R., Velichenko, A., 2016. Electrodeposition of Ni<sup>2+</sup>-doped PbO<sub>2</sub> and physicochemical properties of the coating. *J. Electroanal. Chem.* 774, 88–94.
- Terezo, A.J., Pereira, E.C., 2000. Fractional factorial design applied to investigate properties of Ti:IrO<sub>2</sub>-Nb<sub>2</sub>O<sub>5</sub> electrodes. *Electrochim. Acta* 45, 4351–4358.
- Tomi Ryyänen, K.N., Hämäläinen, Jani, Leskelä, Markku, Lekkala, J., 2010. pH electrode based on ALD deposited iridium oxide. *Procedia Eng.* 5, 548–551.
- Umezawa, Yoshio, Bühlmann, P., Umezawa, Kayoko, Tohda, Koji, Amemiya, Shigeru, 2000. Potentiometric selectivity coefficients of ion-selective electrodes part I. Inorganic cations. *Pure Appl. Chem.* 72, 1851–2082.
- Wang, Jyh-Liang, Yang, Po-Yu, Hsieh, Tsang-Yen, Hwang, Chuan-Chou, Juang, Miin-Horng, Juang, Miin-Horng, 2013. pH-Sensing Characteristics of Hydrothermal Al-Doped ZnO Nanostructures. Hindawi Publishing Corporation *J. Nanomater.* 2013.
- Weber, I.T., Andrade, R., Leite, E.R., Longo, E., 2001. A study of the SnO<sub>2</sub>.Nb<sub>2</sub>O<sub>5</sub> system for an ethanol vapour sensor: a correlation between microstructure and sensor performance. *Sens. Actuat. B* 72, 180–183.
- Winiarski, J., Leśniewicz, A., Pohl, P., Szczygiel, B., 2016. The effect of pH of plating bath on electrodeposition and properties of protective ternary Zn-Fe-Mo alloy coatings. *Surf. Coat. Technol.* 299, 81–89.
- Wu, M.-H., Lee, Yu-Fang, Lin, Chao-Wen, Tsai, Shiao-Wen, Wang, Hsin-Yao, Pan, Tung-Ming, 2011. Development of high-kTm<sub>2</sub>Ti<sub>2</sub>O<sub>7</sub> sensing membrane-based electrolyte-insulator-semiconductor for pH detection and its application for glucose biosensing using poly(N-isopropylacrylamide) as an enzyme encapsulation material. *J. Mater. Chem.* 21 (2), 539–547.
- Xiao-Yu, Xu., Yan, Bing, 2016. An efficient and sensitive fluorescent pH sensor based on amino functional metal-organic frameworks in aqueous environment. *Dalton Trans* 45 (16), 7078–7084.
- Yang, Shu-Ying, Chen, C.-W., Chou, Jung-Chuan, 2012. Investigation on the sensitivity of TiO<sub>2</sub>:Ru pH sensor by Taguchi design of experiment. *Solid-State Electron.* 77, 82–86.
- Yao, Sheng, Wang, Min, Madouz, Marc, 2001. A pH electrode based on melt-oxidized iridium oxide. *J. Electrochem. Soc.* 148 (4), H29–H36.
- Zaki, T., Kabel, Khalid I., Hassan, H., 2012. Using modified Pechini method to synthesize a-Al<sub>2</sub>O<sub>3</sub> nanoparticles of high surface area. *Ceram. Int.* 38, 4861–4866.
- Zhuykov, S., 2009. Morphology of Pt-doped nanofabricated RuO<sub>2</sub> sensing electrodes and their properties in water quality monitoring sensors. *Sens. Actuat. B: Chem.* 136 (1), 248–256.
- Zhuykov, Serge, Kats, E., Kalantar-zadeh, Kourosh, Breedon, Michael, Miur, Norio, 2016. Influence of thickness of sub-micron Cu<sub>2</sub>O-doped RuO<sub>2</sub> electrode on sensing performance of planar electrochemical pH sensors. *Talanta* 146, 517–524.
- Zimer, Alessandro M., Lemos, S.G., Pocrifka, Leandro A., Pereira, E. C., Mascaro, Lucia H., 2010. Needle-like IrO/Ag combined pH microelectrode. *Electrochem. Commun.* 12, 1703–1705.